Candido *et al. Earth, Planets and Space (2018) 70:104*
https://doi.org/10.1186/s40623-018-0875-8

Earth, Planets and Space

FULL PAPER

Open Access

Response of the total electron content at Brazilian low latitudes to corotating interaction region and high-speed streams during solar minimum 2008

Claudia M. N. Candido[1,2*], Inez S. Batista[2], Virginia Klausner[3], Patricia M. de Siqueira Negreti[2], Fabio Becker-Guedes[2], Eurico R. de Paula[2], Jiankui Shi[1] and Emilia S. Correia[2,4]

Abstract

In this work, we investigate the Brazilian low-latitude ionospheric response to two corotating interaction regions (CIRs) and high-speed streams (HSSs) events during the solar minimum of solar cycle 23, in 2008. The studied intervals are enclosed in the whole heliospheric interval, studied by other authors, for distinct longitudinal sectors. CIRs/HSSs are structures commonly observed during the descending and low solar activity, and they are related to the occurrence of coronal holes. These events cause weak-to-moderate recurrent geomagnetic storms characterized by negative excursions of the interplanetary magnetic field, IMF_Bz, as well as long-duration auroral activity, considered as a favorable scenario for continuous prompt penetration interplanetary electric field (PPEF). In this study, we used the vertical total electron content (VTEC) calculated from GPS receivers database from the Brazilian Continuous Monitoring Network managed by the Brazilian Institute of Geography and Statistics. Moreover, we analyzed the F-layer peak height, hmF2 and the critical plasma frequency, foF2, taken from a Digisonde installed at the southern crest of the equatorial ionization anomaly, in Cachoeira Paulista, CP. It was observed that during the CIRs/HSSs-driven geomagnetic disturbances VTEC increased more than 120% over the quiet times averaged values, which is comparable to intense geomagnetic storms. On the other hand, VTEC decreases were also observed during the recovery phase of the storm. Spectral analysis using gapped wavelet technique (GWT) revealed periodicities of 7, 9, 13.5 days, which are sub-harmonics of the solar rotation period, ~ 27 days. These periods in VTEC are closely associated with those observed in solar and geomagnetic indices such as Vsw, IMF_Bz and AE during CIRs/HSSs intervals. We discuss PPEF associated to IMF_Bz reconnection processes and the auroral activity as the most probable causes for the VTEC variations. These results can be of interest for studies related to space weather monitoring, modeling and forecasting, especially during low solar activity.

Keywords: Solar minimum, High-speed streams, Corotating interaction region, High-intensity long-duration continuous auroral activity, Equatorial ionization anomaly, Total electron content

Introduction

Solar cycles 23–24 were characterized by a very unusual quiet and long low solar activity period, which lasted from 2006 to 2010, and it reached a minimum level in 2008 and a minimum in geomagnetic activity in 2009. This peculiar period inspired new interest about the role of low solar activity on different phenomena from several areas of knowledge such as solar physics, magnetosphere, environment, meteorology, aeronomy and space weather (Denton et al. 2008; Gray et al. 2010; Gibson et al. 2009; Schwadron et al. 2011; Burns et al. 2012; Emmert et al. 2010; Solomon et al. 2013; Klenzing et al. 2011;

*Correspondence: claudia.candido@inpe.br
[1] State Key Laboratory for Space Weather, National Space Science Center (NSSC), Chinese Academy of Sciences (CAS), N°1, Nanertiao, Zhongguancun, Haidian District, Beijing 100190, China
Full list of author information is available at the end of the article

Araujo-Pradere et al. 2011). The minimum has also provided an opportunity to study the Sun with new instruments not available before in previous solar cycles (Harvey 2013). In 2008–2009, the sunspot number presented a minimum only comparable to the observed in 1913, much before the beginning of space age. Solar indices presented annual average lower than those observed in the previous solar minimum in 1996. The geomagnetic activity was 30% lower in 2008 and more than 50% lower in 2009 in comparison with the observed in the previous minimum, while energy flux at extreme ultraviolet radiation (EUV) was at least 10% lower in 2008–2009 (Solomon et al. 2013). All these factors played an important role in neutral and ionospheric processes. Emmert et al. (2010) analyzed satellite drag data and found that the thermospheric density was about 30% lower than the expected values. Also, the ionosphere variability during solar minimum has been extensively investigated. The low-latitude ionosphere is continually influenced by several highly variable electrodynamic processes. Coupling processes involving quiet time low-to-high atmosphere interactions (semidiurnal tides, gravity waves, planetary waves) as well as ionosphere-thermosphere-magnetosphere coupling during disturbed geomagnetic conditions (prompt penetration of electric field, ionospheric disturbance dynamo effects) are responsible for high variability of ionosphere system (Fejer 2011). Low solar activity is considered a good period to study these variations without large magnetosphere energy inputs as those associated to interplanetary coronal mass emission (ICMEs). Liu et al. (2012) compared the low-latitude ionosphere to one equatorial region, Jicamarca, during the two last solar minima 1996 and 2008. They found that the plasma densities were lower in 2008 than in 1996 during both daytime and nighttime and suggested the influence of lower EUV levels. Solomon et al. (2013) found global mean ionospheric plasma densities around 15% lower than those observed in 1996, and this decrease was partially attributed to decrease in EUV radiation. Despite the low solar indices, with more than 270 days without sunspots, the Sun was not exactly inactive, as the occurrence of coronal holes has a role in the occurrence of other phenomena. It is well-known that periods of descending activity and even minimum activity in the Sun are associated with a higher occurrence of large and recurrent coronal holes, which corotate with the solar rotation period of ~ 27 days. Coronal holes are dark and low densities regions in the corona characterized by high and open magnetic field line (one side attached to the Sun and the other floating in interplanetary space), which emanates high- and low-speed solar plasma streams. Coronal holes at high solar latitudes are larger during solar minimum and emanate HSSs, which travel in the interplanetary medium with speeds of 500–800 km/s (Tulasi Ram et al. 2012). High-speed structures are emanated by coronal holes and interacts with the low-speed equatorial streams, creating CIRs which corotate with the Sun (Tsurutani et al. 2006). The high oscillatory nature of the IMF_Bz present in these structures and their positive and negative inversions may cause reconnection with the Earth's magnetic field, prompt penetration of interplanetary electric field and other processes such as energetic electrons precipitation, auroral heating and their subsequent processes (Tulasi Ram et al. 2010). As these structures reach the Earth's magnetosphere under distinct ways and strengths and with periods of 27 days and its sub-harmonics, they can be responsible for recurrent low-to-moderate geomagnetic activity and complex responses of the ionosphere. Xystouris et al. (2014) have been classified as 51 high-speed streams in 2008. In this work, we study the variation of the low-latitude ionosphere during two CIRs/HSSs events occurred during this unusual solar minimum year, enclosing an equatorial station and a region around the EIA over Brazilian longitudinal sector. The Brazilian ionospheric region analyzed in this work is characterized by the highest negative declination angle of the planet (at low latitudes) and is surrounded by South American/Atlantic Magnetic Anomaly (SAMA), where the geomagnetic field presents its lowest intensity. Due to its large continental extension, which encloses geomagnetic conjugate points, Brazil is an unique location that enables us to observe distinct ionospheric phenomena. Among them, there are large-scale plasma ionospheric irregularities, or equatorial plasma bubbles, EPBs, originated at equatorial region (Abdu 2005; Abdu et al. 2008; Sobral et al. 2002; Abalde et al. 2009). Besides, it is observed the occurrence of large deposition of plasma at low latitude, referred as the southern EIA crest. The EIA is characterized by high electron concentration at both sides of the magnetic equator around $\pm 15^{\circ}$ magnetic latitude. This scenario is caused by the upward $E \times B$ plasma drift (where E is the diurnal zonal electric field and B the magnetic field), which raises the F-region to higher altitudes. Subsequently the ionization flows by diffusion downward along the magnetic field lines under the action of gravity and pressure gradient forces creating the northern and southern EIA crests. Additionally, processes such as ionospheric scintillations related to plasma irregularities are strongly observed in these regions, being extensively studied due to their spurious effects to the technological systems such as telecommunications and navigation systems (Bhattacharyya et al. 2014). As there are large gradients in plasma densities at low latitudes, it is important to investigate the ionospheric variability during recurrent low-to-moderate geomagnetic storms associated with CIRs/HSSs during

low/moderate solar activity. Plasma depletions and post-midnight irregularities were frequently observed during solar minimum 2008–2009 at the same location around the EIA in Brazil, during June solstice, and they were interpreted as associated to the propagation of mesoscale traveling ionospheric disturbances (MSTIDs) coming from middle latitudes (Candido et al. 2008, 2011). Ionospheric variability at around the EIA in Brazil associated to high-intensity long-duration continuous auroral activity (HILDCAAs), which in turn is connected to the occurrence of HSSs/CIRs, was scarcely studied (Koga et al. 2011; Hajra et al. 2013; de Siqueira Negreti et al. 2017). On the other hand, several authors have contributed to the understanding of the impact of CIRs/HSSs on the global ionosphere (Lei et al. 2008; Liu et al. 2012; Burns et al. 2012; Tulasi Ram et al. 2010; Pedatella and Forbes 2011; Verkhoglyadova et al. 2011, 2013; Wang et al. 2011). Verkhoglyadova et al. (2011) studied the global response of VTEC in the same CIRs/HSSs intervals studied in the present work, using global ionospheric maps (GIMs). They noticed remarkable differences among distinct latitudinal regions, by using the average TEC over each latitudinal range: 0°–30° for low latitude, 30°–50° for middle latitude and 50°–90° for high latitude. However, the VTEC variations during these CIRs/HSSs intervals were analyzed in detail only for the North Hemisphere. This study aims to take advantage of this very quiet scenario provided by the low solar flux during 2008, to investigate the general behavior of low-latitude ionosphere in the Brazilian sector under the impact of CIRs/HSSs-driven weak-to-moderate geomagnetic recurrent storms.

Data and method

We used VTEC variation and others ionospheric parameters such as foF2 and hmF2 taken from a Digisonde installed in Cachoeira Paulista (CP), Brazil, to analyze two CIRs/HSSs intervals in 2008, the solar minimum of the solar cycle #23. VTEC was obtained by global positioning system (GPS) receivers in Brazilian sector, from the equatorial region to the latitudes around the southern crest of the EIA. The data were provided by the ground-based GPS/GNSS receivers network (Brazilian Continuous Monitoring Network, RBMC), managed by IBGE (Brazilian Institute of Geography and Statistics), in Brazil (Web site: www.ibge.gov.br/home/geociencias/geodesia/rbmc/rbmc_est.shtm). The satellite navigation data were provided by the International GNSS Service, IGS (Web site: http://igscb.jpl.nasa.gov). The vertical TEC values were calculated using the Nagoya Model (Otsuka et al. 2002) by converting the slant TEC, which depends on the satellite elevation angle. Only elevation angles greater than 30 degrees were selected. The instrumental biases from satellites and receivers were also removed by a technique based on the least squares fitting procedure as described by Otsuka et al. (2002). The VTEC variation during the selected intervals was calculated by the subtraction of the averaged VTEC over the five quietest days from the disturbed VTEC value ($\Delta VTEC = VTEC - VTEC_{AV5QD}$). The VTEC variation was analyzed for the latitudinal range enclosing Brazilian sector, from equatorial region to around the southern crest of EIA, 0°–30°S geographic latitude or 0°–21° geomagnetic latitude, around the longitude ~ 45°W. For a more detailed analysis, we included the day-by-day VTEC variation using VTEC calculated by the method developed at Boston College (Seemala and Valladares 2011) for some representative stations separately. Percentual VTEC deviation was also calculated related to $VTEC_{AV5QD}$, as follows: $VTEC_{DEV\%} = (VTEC - VTEC_{AV5QD})/VTEC_{AV5QD} \times 100\%$. Additionally, we analyzed other ionospheric parameters such as hmF2 (F-layer peak height) and foF2 (critical plasma frequency), where foF2 is related to F-layer plasma density by $NmF2 = 1.2 \times 10^4 (foF2)^2$, taken from data collected by a Digisonde installed in CP (23.4°S, 45°W, dip lat: 32.7°S) which is useful for comparison. Digisonde data were manually processed using the software SAO Explorer provided by the University of Massachusetts—Lowell group (Reinisch et al. 2005). Six representative stations from equatorial to the south edge of EIA are listed in Table 1 (SALU, FOR, GVAL, UBAT, CP, SMAR) and shown in the Brazilian map in Fig. 1 as blue circles (GPS stations) and a red circle (Digisonde station). Two selected intervals were studied: March 24 to April 04, 2008, enclosed in the Whole Heliospheric Interval (WHI) and the period April 19 to

Table 1 Coordinates of six representative stations in Brazil used for TEC and Digisonde data

Station	Instrument/technique	Latitude	Longitude	Dip lat
SALU (Sao Luis)	GPS/GNSS VTEC SPECTRAL analysis	2.6°S	44.2°W	8.7°S
FOR (Fortaleza)	GPS/GNSS receiver	3.8°S	38.4°W	13.1°S
GVAL (Governador Valadares	GPS/GNSS receiver	18.5°S	41.4°W	31.8°S
UBAT (Ubatuba)	GPS/GNSS receiver	23.5°S	45.4°W	34.9°S
CP Cachoeira Paulista (CP)	Digisonde DPS4	23.4°S	45.0°W	32.7°S
SMAR (Santa Maria)	GPS/GNSS receiver	29.2°S	53.2°W	35.9°S

Fig. 1 Brazilian map with the locations of the stations used in this work. Blue circles: five representative GPS stations for timeline VTEC variation taken from RBMC network managed by IBGE. Red circle: Digisonde station. Blue Line: geomagnetic equator

April 30, 2008 (Verkhoglyadova et al. 2011, 2013; Wang et al. 2011) which is a recurrent geomagnetic storm related to the first event in March. However, this second period is a recurrent and less intense geomagnetic storm related to the same coronal hole. We also performed spectral analysis using gapped wavelet technique (GWT) as described by Klausner et al. (2013). This technique was chosen because it reduces the effects of gaps in time series (an advantage for some periods of VTECs measurements gaps) and boundary effects associated with the finite length of time series. Additionally, this technique suppresses the low and high noise frequencies, better estimating the frequencies of the signal. For more details, see Klausner et al. (2013) and references therein. We applied the GWT to identify periodicities in VTEC and compare to other known solar, interplanetary and geomagnetic indices/parameters. Klausner et al. (2016) performed a spectral analysis of AE, Kp and Dst using GWT and found a periodicity of 27 days, and the sub-harmonics of Sun rotation, 9 and 13.5 days also associated with CIRs/HSSs. The solar/interplanetary and geomagnetic parameters used in this work were obtained from the National Space Science Data Center's OmniWeb (http://omniweb.gsfc.nasa.gov), with a resolution of 5 min.

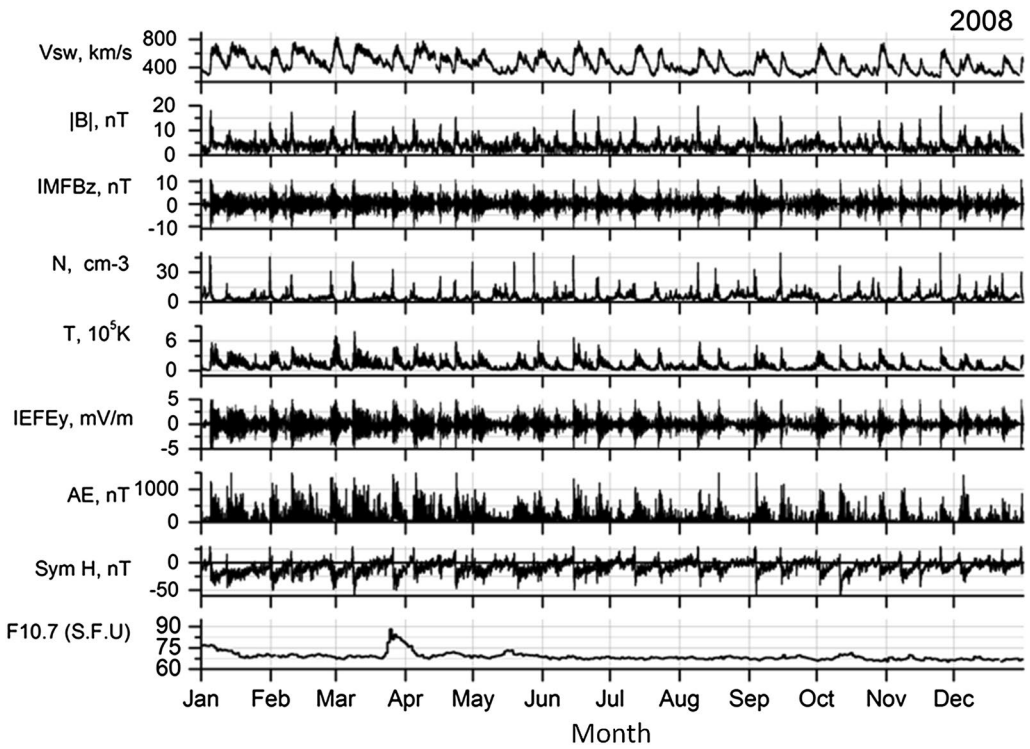

Fig. 2 Solar, interplanetary and geomagnetic indices and parameters for the solar minimum in 2008

Results and discussion

HSSs in 2008

Figure 2 shows the annual variation of solar and geomagnetic indices, and interplanetary parameters used to identify CIRs/HSSs and their effects on geomagnetic parameters for the solar minimum year 2008. Panels from top to bottom present the variation of the following parameters: solar wind speed, Vsw (km/s); solar wind magnetic field strength, $|B|$; north-south component of the interplanetary magnetic field (nT), IMF_Bz (nT); proton density, Np (cm-3); proton temperature, T (K); dawn-to-dusk interplanetary electric field IEF_Ey (mV/m); auroral electrojet index, AE (nT); 1-min time resolution intensity of storm time ring current, Sym H (nT). Solar wind speeds reached typical values of high-speed streams, ~ 600–800 km/s during the CIRs/HSSs intervals, therefore over the average solar wind speed which is ~ 400 km/s. These intervals are marked by a sudden rise in Vsw, Tp and decrease in density, Np. It is remarkable the high oscillatory nature of some parameters such as interplanetary, magnetic field IMF_Bz, and interplanetary electric field, IEF_Ey, as well as the auroral index, AE, which is all associated to Alfvén waves within the CIRs. AE variations are indicative of auroral activity likely caused by Joule heating or by energetic particle precipitation. During these intervals, the continuous auroral activity should obey some criteria to be considered HILDCAAs (Tsurutani et al. 2006). The 10.7-cm solar flux presented in the bottom panel is typical of deep low solar activity, although there is a more significant peak in March, probably due to the occurrence of two small C and M—class solar flares (see Verkhoglyadova et al. 2011). Another important feature is that the maximum of Sym H did not exceed 60 nT, while $|B|$ are typical ~ 20 nT. On its turn, IEF_Ey are typically ~ 5 mV/m, very distinct from those associated with CMEs, which can be more than 40 mV/m. The impact of HSSs on the ionosphere may present a variety of responses since the solar wind speed increases until the end of the geomagnetic storm recovery phase, which can last from 3 to 10 days.

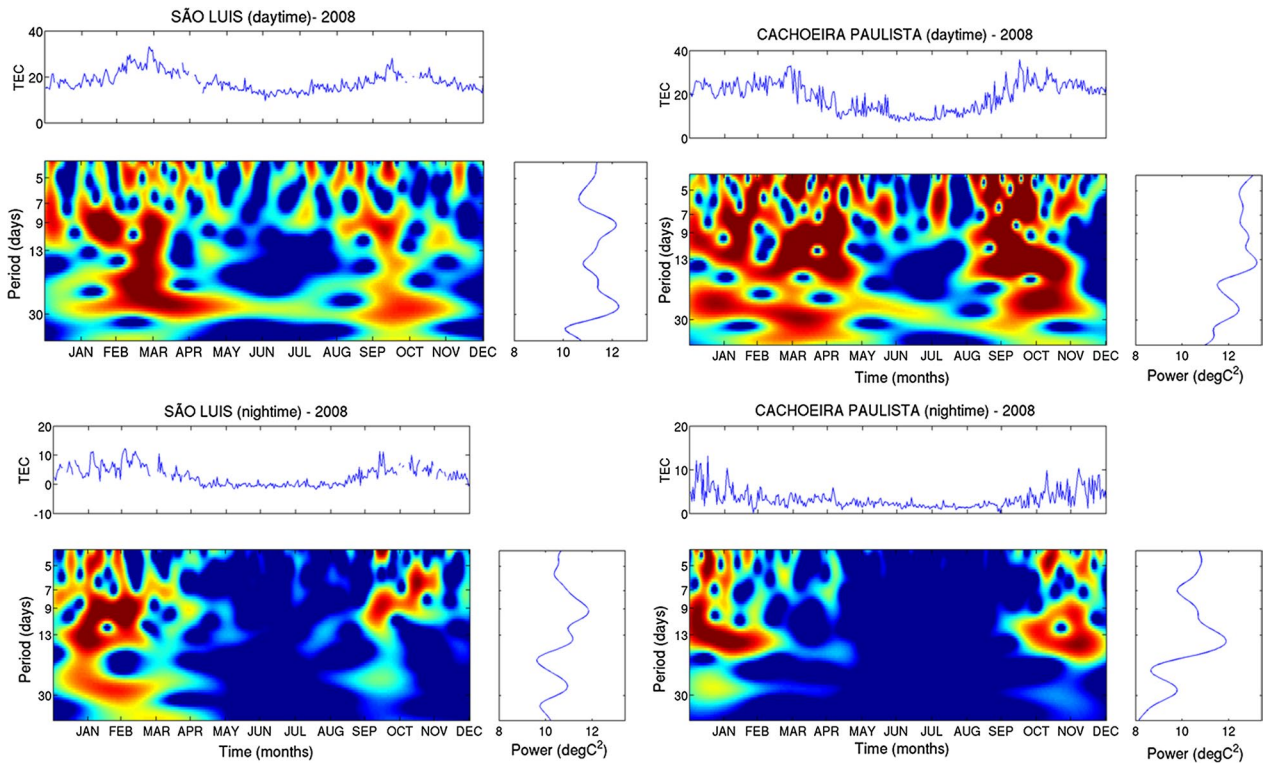

Fig. 3 Diurnal (top panel) and nocturnal (bottom panel) annual VTEC variation and Gapped Wavelet Spectra in 2008. Left panel: quasi-equatorial region, Sao Luis, SALU. Right panel: Cachoeria Paulista, CP

Besides, the Alfvén waves in the magnetic field of CIRs are observed in the components of the interplanetary and geomagnetic indices, as continuous input/pumping of energy in the magnetosphere which causes a variety of interactions and responses at high-, middle- and low-latitude ionosphere.

Spectral analysis of VTEC

Figure 3 shows the annual variation of VTEC during 2008 and its spectral analysis by GWT for two representative Brazilian regions, in Sao Luis, SALU (a quasi-equatorial station), and at Cachoeira Paulista, CP (around the south crest of EIA). Spectral analysis is performed for the annual VTEC at both stations and separately for daytime (09:00 to 21:00 UT) and nighttime (21:01 to 08:59 UT), where UT = LT + 3 h. It is possible to observe the high day-to-day variability of the VTEC in both regions and semiannual variation with peaks during equinoxes (top panel). In 2008, VTEC presented maximum values not higher than 35 TECU. From the spectral analysis, periods of 27, 16, 13.5, 9, 7, and 5 days were observed, with some few differences from daytime to nighttime. During daytime periods of 7, 9, 16 and 27 days are observed at equatorial region, while around the southern crest of EIA, the most evident periods are 7, 9, 13.5, 27. At night the usual periods are 9 and 13.5 days for both regions. The power spectrum is stronger in equinoxes at CP, which is possibly associated with the higher plasma density in this season. On the periodicities causes, it should be addressed they are associated with solar, interplanetary and geomagnetic periods. Wang et al. (2011) studied the periodicities of ionospheric parameters such as NmF2 at distinct latitudinal regions during the WHI period compared to the periods observed in solar, interplanetary and geomagnetic indices and parameters. They observed that periods of 9 and 13.5 days are mainly associated with the geomagnetic activity or with variations of IMF_Bz and Vsw, which consequently appear in IEF_Ey and PPEF. In this present study, periods of 5, 7, 9.5 and 13.5 are observed in VTEC parameters at the geomagnetic equator and over the

south crest of EIA. These periods are seen in Fig. 3, especially in the equinoxes. Periods of 5 and 13.5 are accepted as associated mainly to variations of IMF_Bz (Wang et al. 2011). As mentioned by Tulasi Ram et al. (2012), the periods observed in many parameters and indices are mostly the sub-harmonics of the solar rotation (~27 days) which means that they are associated to SW energy injection in the magnetosphere by CIRs/HSSs. So, it is plausible to consider that the periods observed in both regions can be a result of the action of PPEFs which strength the F-layer vertical drift $E \times B$, leading to the fountain effect and the transport of the plasma to higher latitudes, forming a stronger EIA. Periods of 16 days were also observed at equatorial region, and the possible explanation for their occurrence is the occurrence of planetary waves at ionospheric heights in this region.

Period of March 24 to April 04

The interplanetary parameters, geomagnetic and solar indices for the first HSS interval analyzed (March 24–April 04) are shown in Fig. 4. Solar wind velocity, Vsw, presents an increase to around 640 km/s on March 26, peaks on March 28 and recovers to mean values ~400 km/s only five days after, on March 30. Sharp increases in the interplanetary magnetic field, $|B|$, and of the plasma density, Np, are observed which represent the passage of a CIR. IMF_Bz and IEF_Ey (IEF_Ey = − Vp × Bz) are highly oscillatory as expected for HSSs intervals, associated to Alfvén waves present in CIR magnetic field. In this interval, it is also observed intense auroral activity (AE ≥ 1000 nT), which obey criteria as those proposed for HILDCAAs events (Tsurutani et al. 2006). Sym H reaches its first minimum, ~ − 50 nT on March 26 at ~19:30 UT. The solar flux represented by the index F10.7 presents intensification during the interval, probably due to a contribution of a small solar flare, classes M and C, as reported by Verkhoglyadova et al. (2011). The recovery phase lasts, at least, until April 02. The VTEC variation for each day of this interval is shown in Fig. 5, for four selected latitudes from around the equatorial region, FOR, to the south edge of the EIA, SMAR (see Table 1). The red line represents the VTEC for each day while the gray line is the average of VTEC during the five quietest days in March, $VTEC_{AV5QD}$. It is observed an

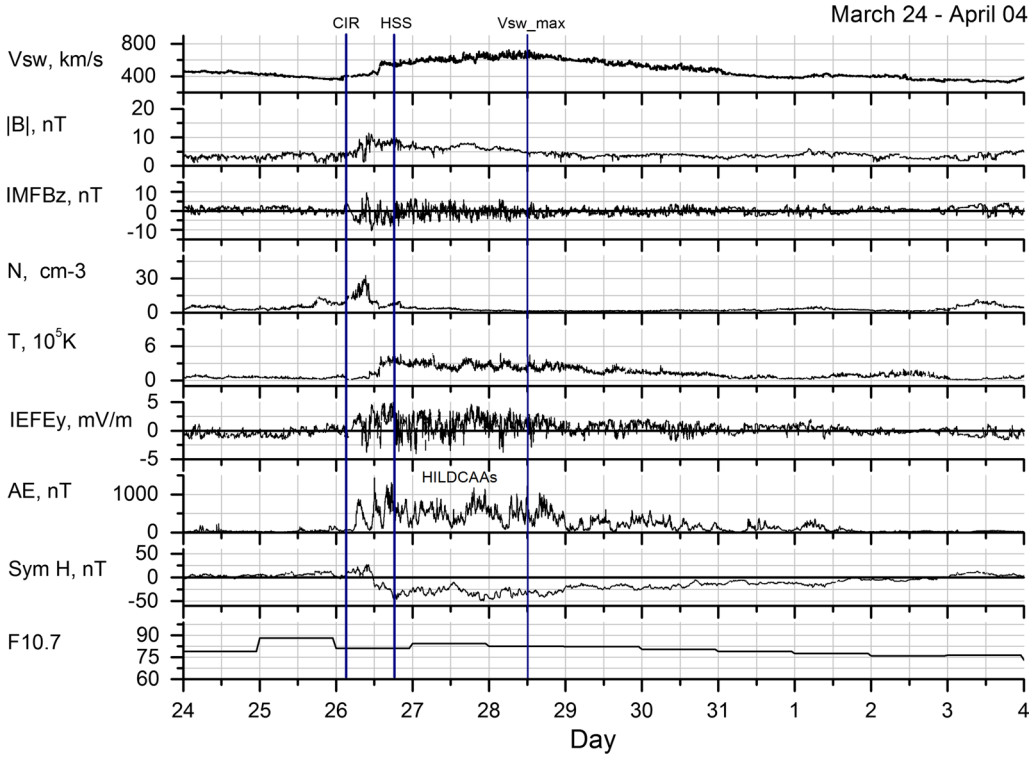

Fig. 4 Solar, interplanetary and geomagnetic indices and parameters for the interval March 24 to April 04

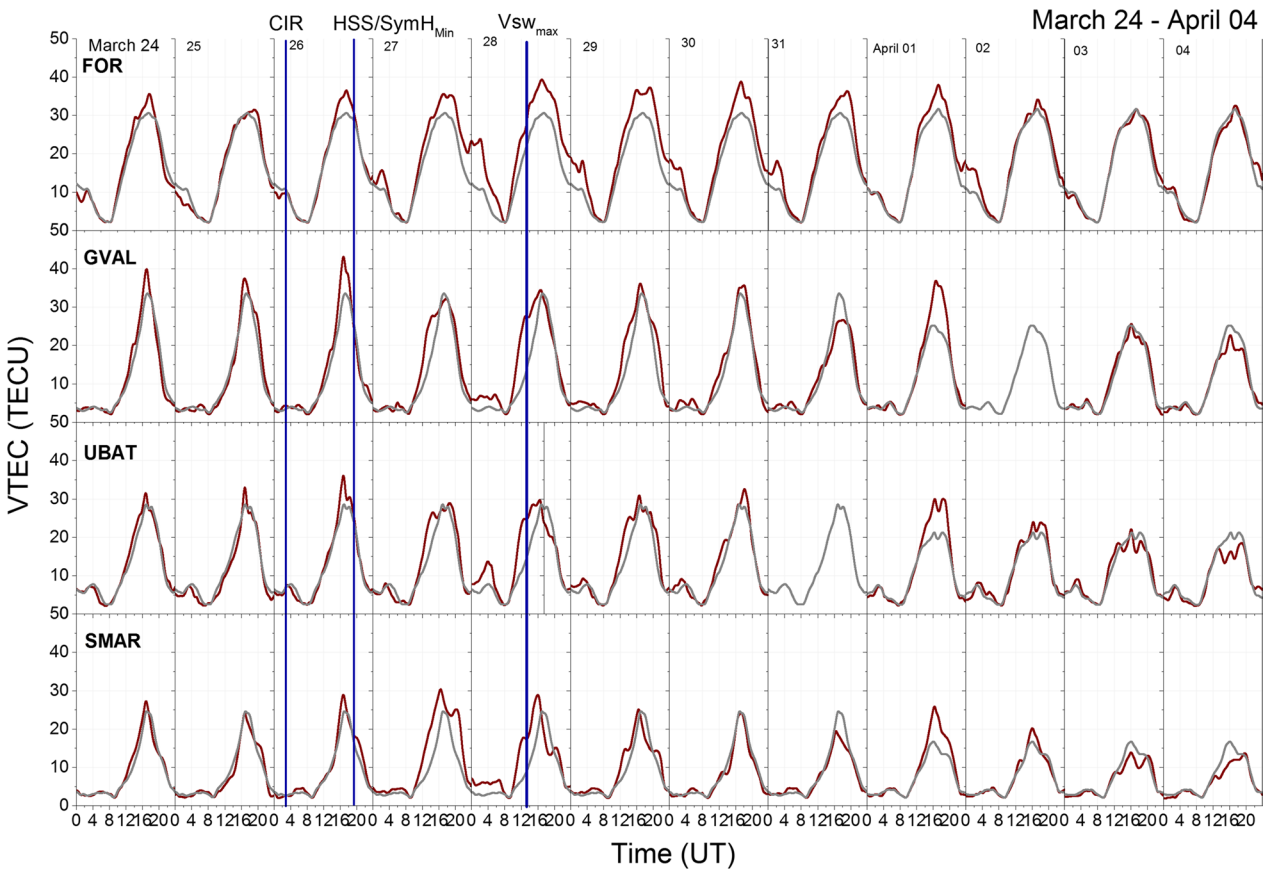

Fig. 5 VTEC variation from March 24 to April 04 in four latitudes in Brazil for the stations FOR, GVAL, UBAT, SMAR. Red: VTEC, Gray: VTEC$_{AV5QD}$

increase in VTEC at all stations since the beginning of the storm until the recovery phase on April 02.

Figure 6 presents the percentage deviation of VTEC for the same interval. It is noticed a percentual deviation of VTEC of more than 120% for several days during the HILDCAA interval, for diurnal and nocturnal periods. The high oscillatory behavior of IMF_Bz and IEF_Ey and the continuous injection of energy possibly cause effective Prompt Penetration Interplanetary Electric Field, PPEF, which are responsible for leading the F-layer to a higher altitude at equatorial regions, and favor the increasing of equatorial VTEC and subsequently the formation of a stronger EIA at low latitudes. As it is well-known, this is only a small fraction of the VTEC variations observed during intense storms related to CMEs, which can reach 300% or more (Mannucci et al. 2009). However, it is significant if we consider that it was observed during solar minimum, 2008, when solar fluxes were very low (mean F10.7 ~ 70 SFU) and intense geomagnetic storms were almost absent. Besides, percentual deviations of more than 120% are seen for several days after the beginning the CIR-driven storm.

For a larger latitudinal view of the ionospheric response at Brazilian sector, we present the VTEC variation for the same interval, in Fig. 7, covering the latitudinal range 0°–30° (0°–21°) geographic (geomagnetic latitude). The south crest of EIA formation is seen before the beginning of the event, around 18:00 UT. However, as the storm develops and Sym H peaks at ~ 19:30 UT (Fig. 4), an intensification of nighttime VTEC values (ΔVTEC > 0) at around 15° latitude is observed which spreads to higher latitudes (until ~ 30° geographic latitude) during the day and stays at the same level until dawn. The intensified formation of the EIA is seen until April 02, after which

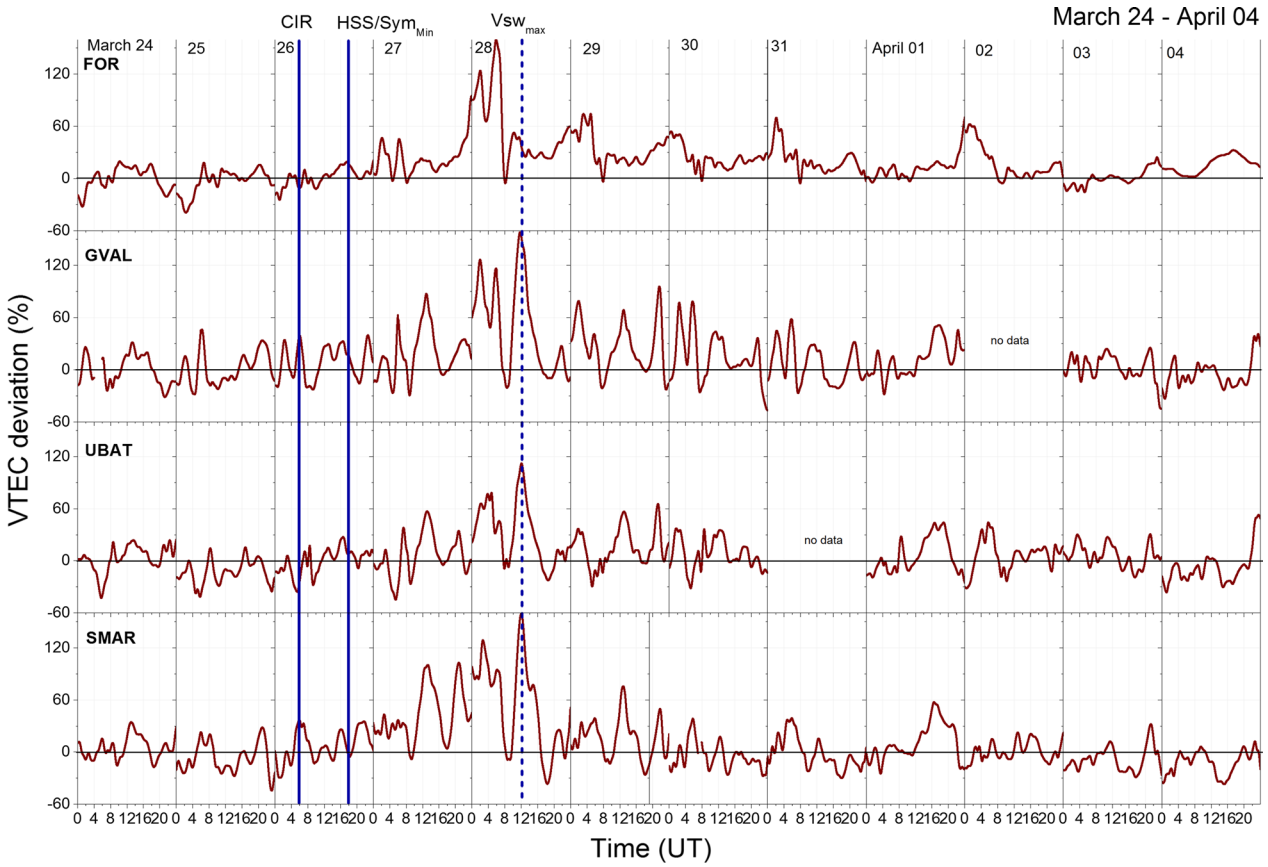

Fig. 6 Percentage VTEC deviation for the interval March 24 to April 04

depletion in ΔVTEC is observed for 2 days. The recovery phase of this storm was marked by intense auroral activity, HILDCAA, and continuous oscillations of IMF_Bz and IEF_Ey, that could be trigger PPEF which is considered to be responsible for the stronger EIA formation.

The diurnal variation of the F-layer peak height, hmF2, and the F-layer critical frequency, foF2, taken from Digisonde measurements installed at Cachoeira Paulista, from March 24 to April 04 is shown in Fig. 8. It is observed that just after the beginning of the storm, on March 26 until the morning of March 27, hmF2 is higher than the $hmF2_{AV5QD}$. This uplift occurs ~ 1.5 h before the intensification of foF2 (bottom panel). The VTEC peak is also delayed by ~ 2 h which is observed for all 4 days, until March 29. We should address the factors possibly related to the F-layer uplift. It is known that auroral activity may trigger several processes such as global thermospheric heating and expansion which affect the ionospheric density, as well as disturbance dynamo (DD) processes. The complex circulation wind system, in which the quiet time meridional wind component is close to zero in equinoxes at equatorial region (Balan et al. 2009; Batista et al. 2017), may also be disturbed during geomagnetic activity, even if it is not intense. Balan et al. (2009) and Batista et al. (2017) pointed out that the action of disturbed equatorward meridional winds is most probable to contribute to the increase in the ionization at low latitudes. Besides, we should point out that a combination of nonlinear interactions during these storms might be considered. As it is seen in Fig. 4, there is a continuous pumping of energy associated to the oscillatory southward IMF_Bz excursions and prompt penetration of IEF_Ey, also associated to long-lasting auroral activity, seen as a HILDCAA event. These conditions favor PPEF processes to the

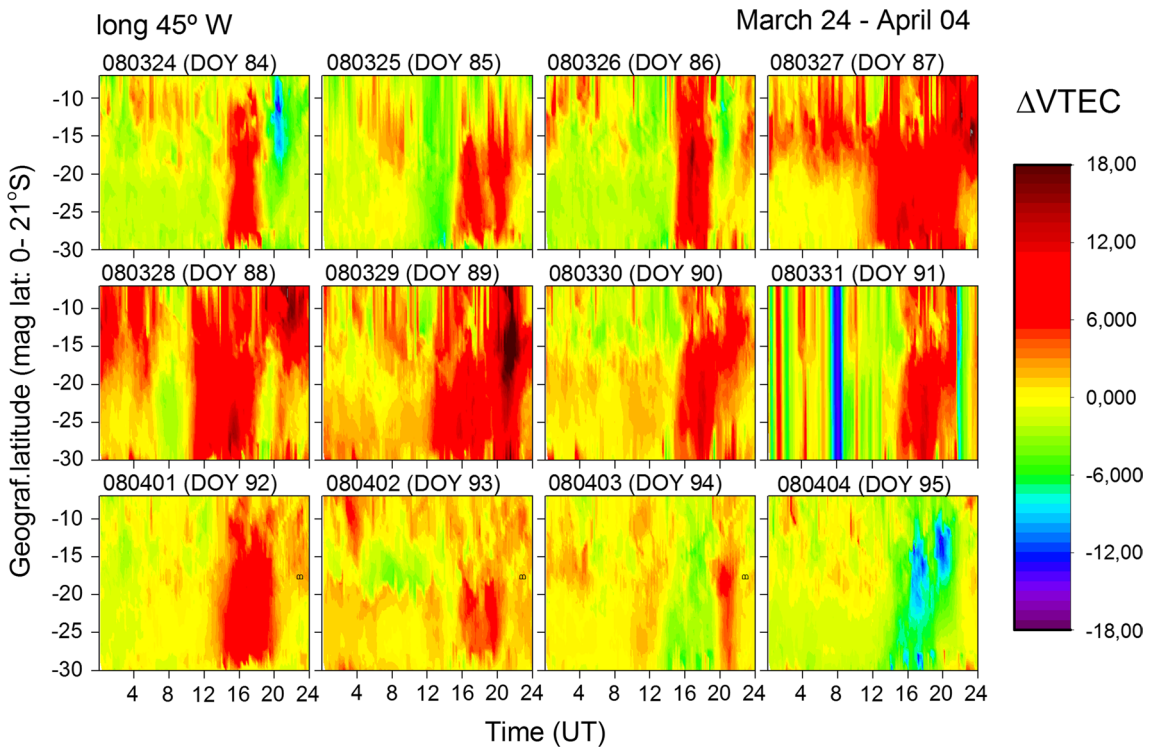

Fig. 7 ΔVTEC variation during the interval March 24 to April 04 at the Brazilian low latitudes, from 00:00 to 24:00 UT, where UT = LT + 3 h

equatorial region, which reinforces the vertical $E \times B$ drift and elevates the F-layer to higher altitudes, distributing plasma to higher latitudes by diffusion due to gravity and gradient pressure forces, resulting in a stronger fountain effect at low latitudes and keeping the ionization at high altitudes at the equatorial region.

Period of April 19 to April 30, 2008

The second period analyzed in this work, referred as "after-WHI" starts on April 19 and ends on April 30. The solar, interplanetary and geomagnetic parameter conditions under which the ionospheric variation occurs are presented in Fig. 9. This event is a recurrent geomagnetic storm associated with the previously studied case of CIRs/HSSs on March, 26. The solar wind increases from ~ 400 to ~ 680 km/s on April 23 at 16:26 UT (13:26 LT). The IMF_Bz, IEF_Ey and Sym H variations are highly oscillatory, as expected for HSS/CIRs related-storms associated with Alfvén waves. This storm recovers to quiet geomagnetic conditions after five days. Minimum Sym H reaches -47 nT and recovers to its quiet condition on April 28. The VTEC variation for this interval is shown in Fig. 10, for four latitudinal selected stations encompassing the longitude of 45°. It is noticed that for the initial phase of the storm, on April 23, which coincides with CIR, Sym H reaches ~ − 43 nT, and VTEC values are higher than the 5QD_VTEC, especially around the southern crest of the EIA, as observed at GVAL, UBAT, and SMAR. No significant changes are observed at equatorial region, at FOR. During the main phase of the storm, which lasts ~ 1 day, it is also observed continuous oscillations in IMF_Bz and IEF_Ey, and in AE. Vsw peaks at ~ 19:30 UT. The continuous IMF_Bz negative excursions and positive IEF_Ey observed in Fig. 9, simultaneously to the VTEC intensification at low latitudes suggest a possible and effective PPEF to low latitudes, which would raise the F-region to higher altitudes and distributes the plasma to higher latitudes to form a stronger EIA. Unfortunately, there are no ΔH data in Brazilian sector for this period, which could be used to show

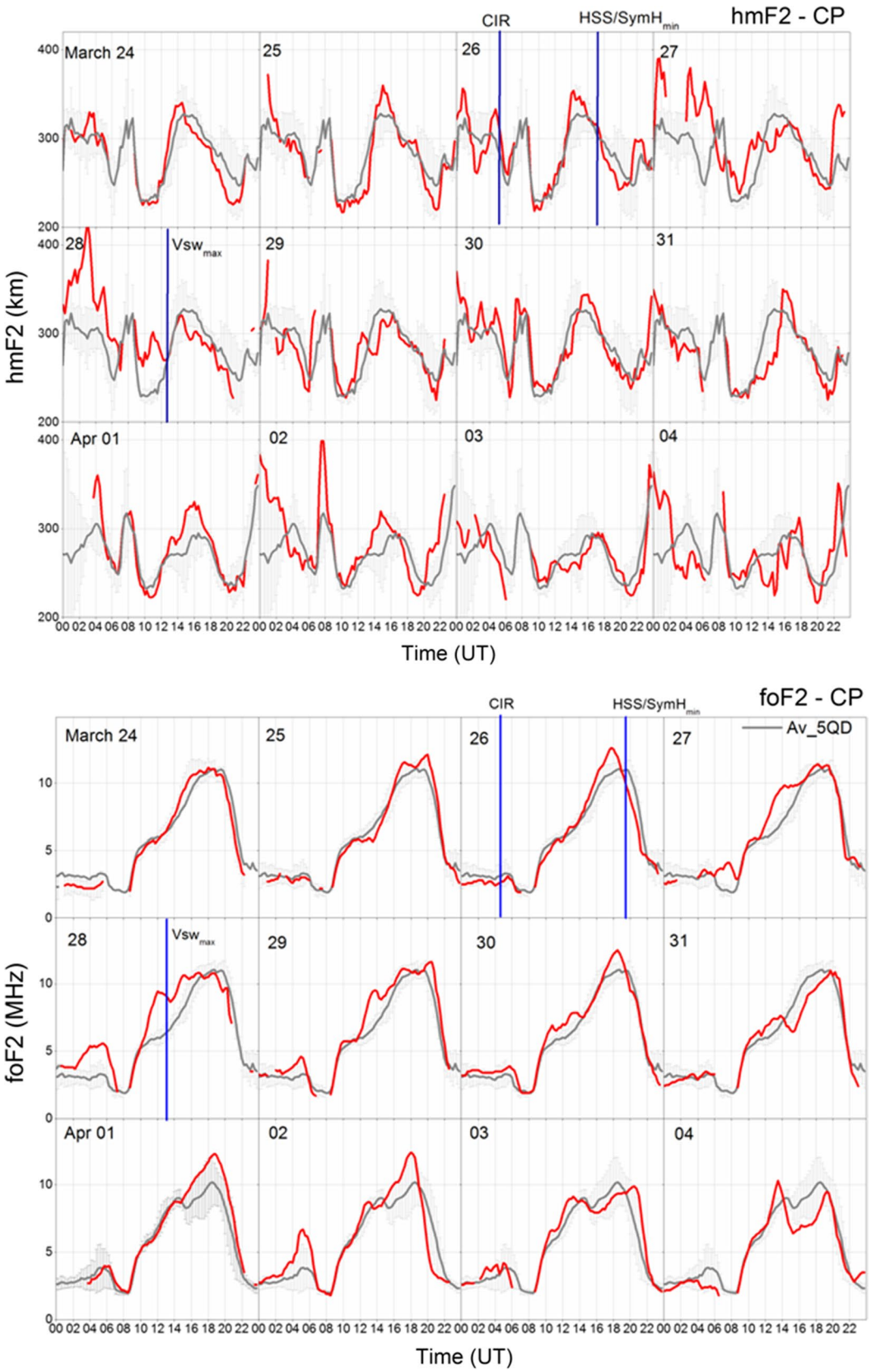

Fig. 8 hmF2 (top panel) and foF2 (bottom panel) variation for the interval March 20 to April 04 taken from Digisonde measurements at CP

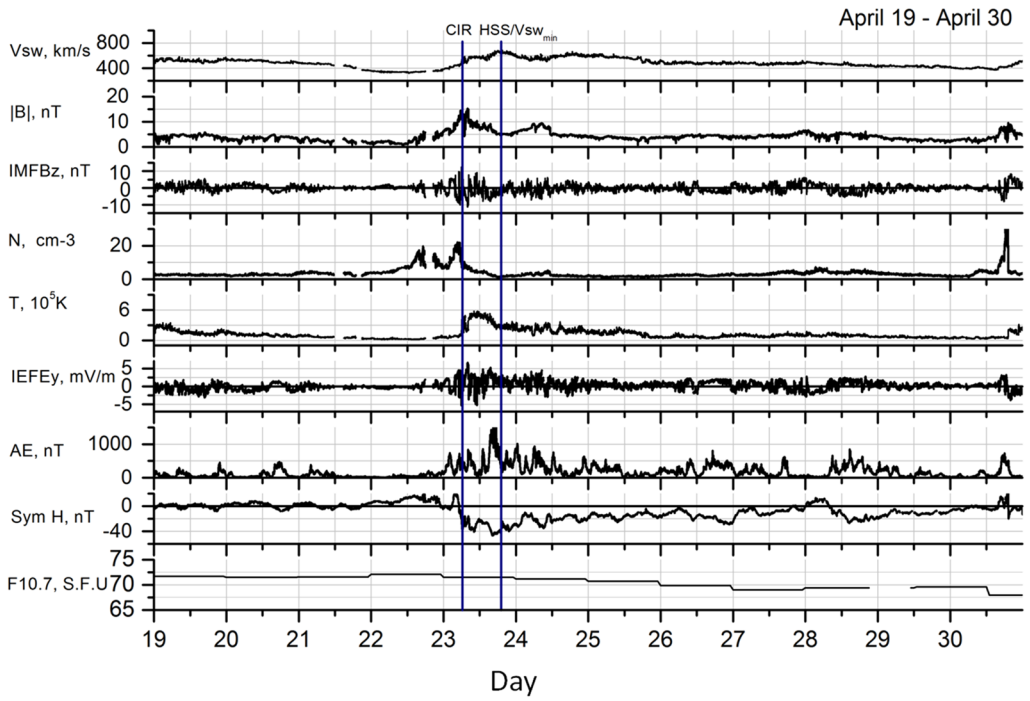

Fig. 9 Solar, interplanetary and geomagnetic indices and parameters for the interval April 19 to April 30, 2008, referred as after WHI period

the local effects of PPEF. On the other hand, we should consider that the intensified VTEC around the southern crest of EIA can also be influenced by disturbed winds which affect more the low latitude than the equatorial ionosphere. The percentual VTEC deviation is shown in Fig. 11. It is noticeable that the low-latitude variability is higher than over the equatorial region. Deviations of ~ 100% are observed at low latitudes, as seen in the bottom panel, at SMAR. For the other stations, the deviations at the same time are around 50% during the main phase of the storm.

For completeness, we present the ΔVTEC variation for the same interval, in Fig. 12, covering the range of 0°–30°S (0°–21°S) geographic/geomagnetic latitudes, for 0–24 UT (where UT = LT + 3). High day-to-day variability is observed. One day before the storm, on April 22, there is a decrease in VTEC in comparison with the quiet time VTEC around the time of occurrence of the EIA, ~ 19:00 UT. However, on April 23, at the beginning of the storm, there is an intensification of VTEC (ΔVTEC > 0) which is in agreement with the low-latitudes results for observations in the Northern Hemisphere, reported by Verkhoglyadova et al. (2011). The recovery phase seems to start on April 24, however, on April 26 it is observed a new increase in VTEC, peaking around 19:00 UT (16 LT). This intensification is not associated with PPEF or auroral activity, as it is observed in Fig. 9 (quiet time IMF_Bz, IEF_Ey or AE). The stronger EIA at this day is possibly due to local effects or even to the local action of gravity waves and needs further investigation.

Bite-outs at low latitudes

A striking point in this work is the observation of noon-time (~ 15:00 UT or ~ 12:00 LT), "bite-outs" or depletions, in the ionospheric parameters, VTEC and foF2, at the low-latitude region, in April (see Figs. 5, 8, 10 and 13). These noon-time "bite-outs" are not associated with the geomagnetic storm or to PPEFs. "Bite-outs" are seen in electron density generally occurring at equatorial region and are explained by processes related to E × B vertical

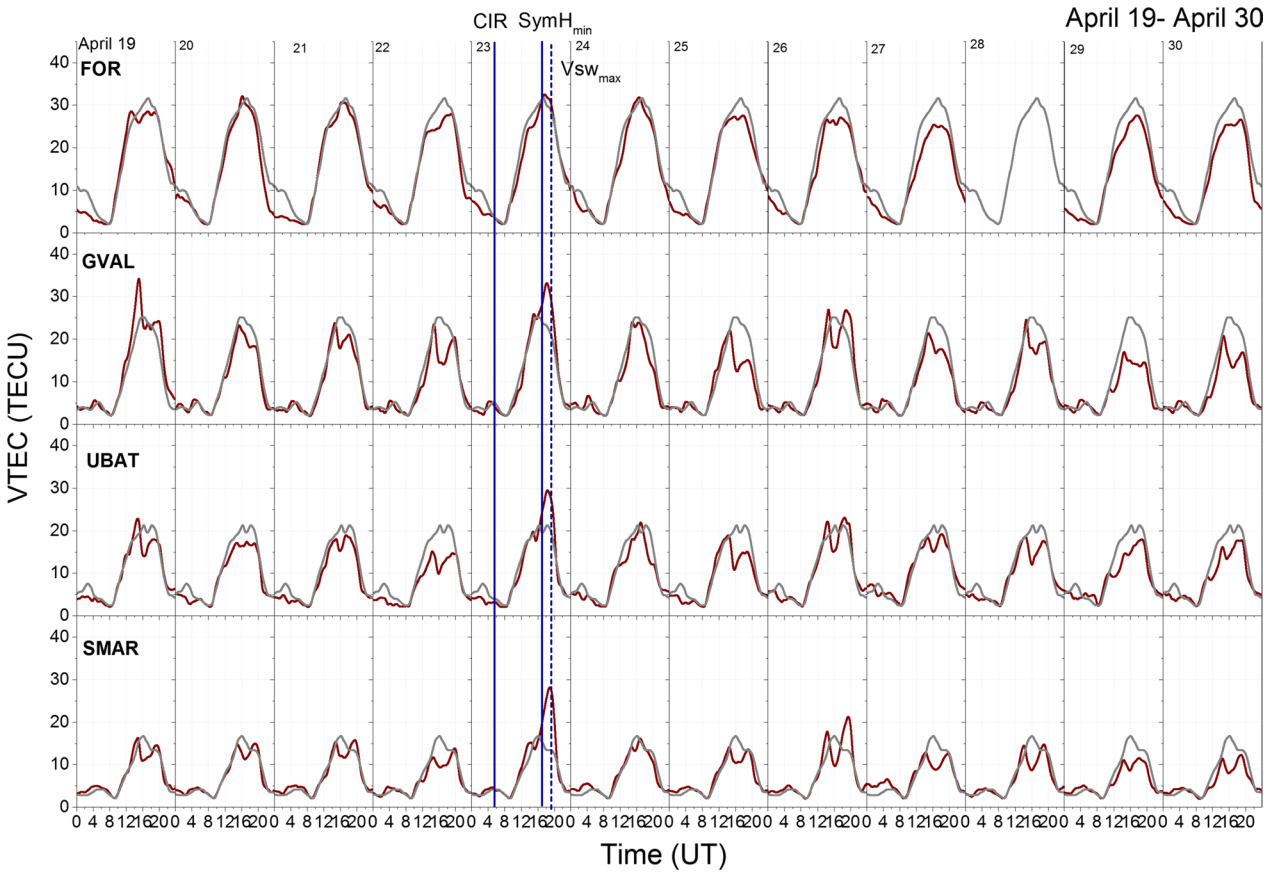

Fig. 10 VTEC variation from April 19 to April 30 from four latitudes in Brazil for the stations for the stations FOR, GVAL, UBAT and SMAR. Red line: VTEC, Gray line: $VTEC_{AV5QD}$

drifts, which raise the F-layer to higher altitudes. As described by Venkatesh et al. (2016) and Rajaram and Rastogi (1977), the rise of the F-layer to higher altitudes is followed by the vertical expansion of the ionosphere and decrease in the F-layer peak electron density at noon-times (15–16 UT). At equatorial region, bite-outs are usually observed in foF2 but are not seen in VTEC, as mentioned by Lee (2012). In this work, they are observed at distinct low-latitude sites but not close to the equator. The processes involved in the development of bite-outs in the equator cannot explain those at low latitudes during the studied interval. To analyze the causes of the "bite-outs" in foF2, we verified the local response over the EIA, in Cachoeira Paulista, CP, taken from a Digisonde data. Notice that CP and Ubatuba are nearby located stations, separated by ~ 85 km, therefore the Digisonde and VTEC data obtained from these sites can be compared to each other.

Figure 13 presents the variation of hmF2 and foF2 from April 19 to 30. The quiet time "bite-outs" generally occurs at ~ 16:00 UT (13:00 LT) in foF2 and the peaks are observed at ~ 14:00 and at 18:30 UT, similar to what is observed in VTEC at low latitudes (see Fig. 10). Additionally, on April 23 (geomagnetic disturbed day), foF2 is not so higher than the $foF2_{AV5QD}$, although it is ~ 60% higher than the previous day (quiet day). The same behavior is seen in hmF2. When comparing the VTEC on the same day presented in Fig. 10 (VTEC UBAT), it is observed that there is a delay of ~ 2 h between hmF2

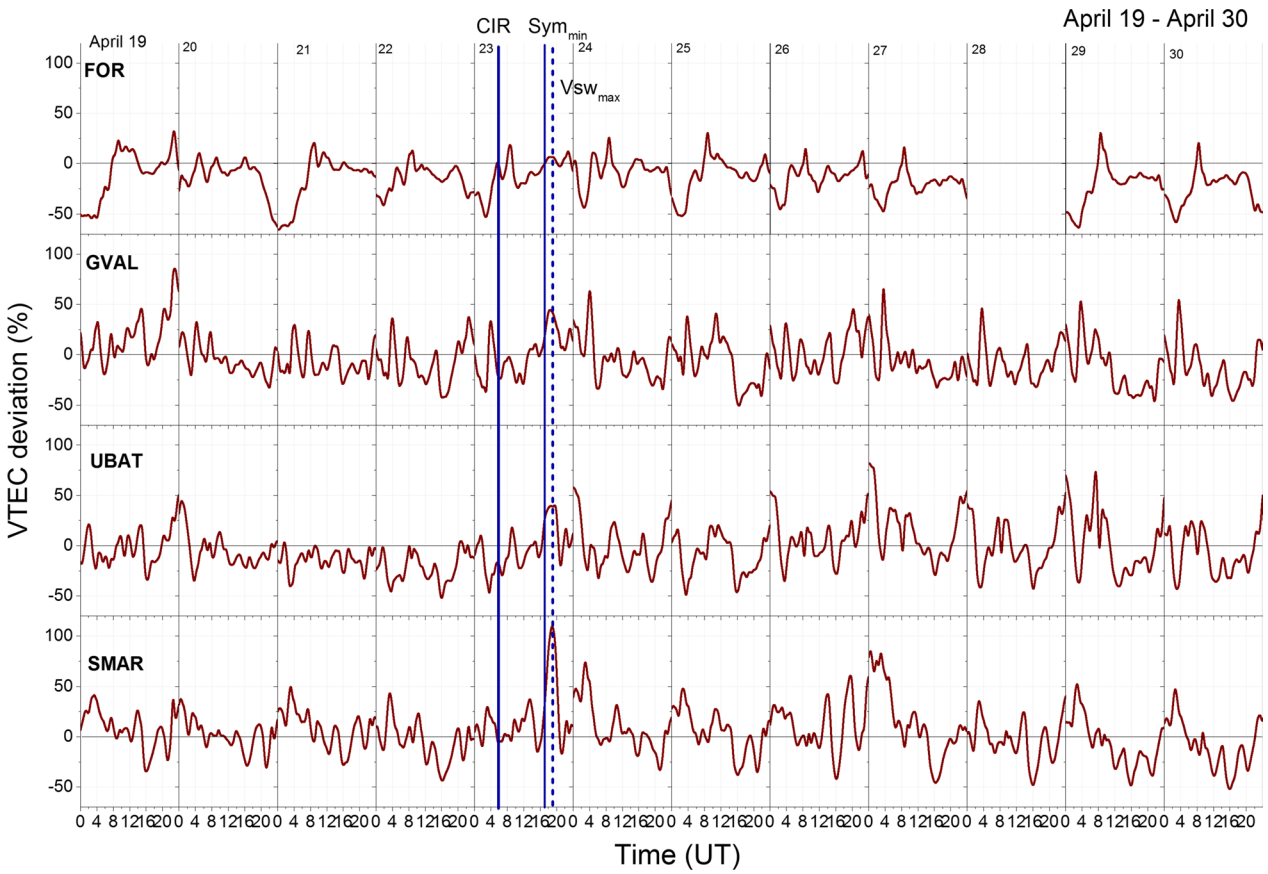

Fig. 11 Percentage VTEC deviation for the interval April 19 to April 30

peak, at ~ 16:00 UT (13:00 LT) and VTEC, at ~ 18:00 UT (15:00 LT), while foF2 and VTEC peaks are in phase.

We applied the same approach used by Venkatesh et al. (2016) to analyze the evolution F-layer behavior, through the ionospheric densities profiles taken from Digisonde data at CP. In their study, the authors examined the variation of hmF2 and NmF2 in 2 days.

Figure 14 shows the F-layer density profiles for 3 days: April 22 (the quiet day before the storm), April 23 (disturbed day), and April 26 (recovery phase). The profiles show that as the ionosphere contracts/expands (lower/higher half-height thickness), the NmF2 increases/decreases on April 23, as seen on the topside of the curve. As the hmF2 is kept at high altitudes, where the recombination is lower, NmF2 increases. It is noteworthy to address the differences observed between the quiet and disturbed day, April 22 and 23, respectively. In Figure 13, the top panel shows that hmF2 on April 23 is higher than in the other days, at ~ 16:00 UT. Besides, the half-height thickness seen in Fig. 14 is also lower than the other days between 17:00 and 18:00 UT, which show a more contracted and denser ionosphere. In this case, it is possible that a disturbed equatorward meridional wind system can have a role in keeping the F-layer at high levels which lead to higher VTEC, creating an additional bite-out at ~ 12:00 UT (09:00 LT).

Conclusions

In this work, we studied the influence of HSSs/CIRs events on the low-latitude ionosphere in Brazil, during solar minimum in 2008. For this purpose, we used VTEC and other parameters such as foF2 and hmF2 taken from

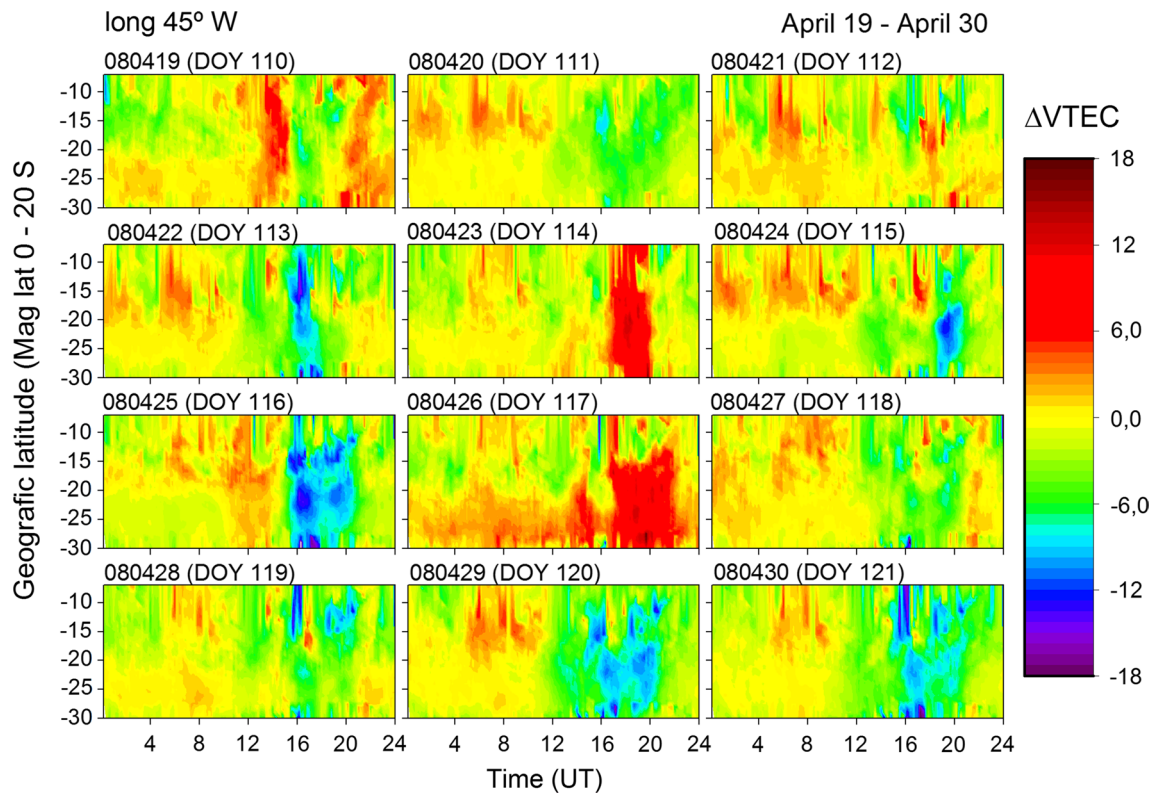

Fig. 12 ΔVTEC variation during the interval April 19 to April 30 ("after WHI" period) at the Brazilian low latitudes, from 00:00 to 24:00 UT, UT = LT + 3 h

Digisonde installed close to the southern crest of EIA. Additionally, we performed spectral analysis using GWT.

Our primary results are summarized below:

1. Solar minimum 2008 was a very unusual period, marked by the occurrence of several HSSs/CIRs events, generally followed by HILDCAAs intervals (auroral activity), as shown in Fig. 2. The solar, interplanetary and geomagnetic parameters presented a very oscillatory behavior related to the presence of Alfvén waves in CIRs.
2. Spectral analysis of VTEC at the equatorial region and over the southern crest of EIA present periods compatible with those exhibited by the solar, interplanetary and geomagnetic parameters. This result revealed a close association between the disturbed VTEC and the drivers related to CIRs, HSSs and HILDCAAs events (Wang et al. 2011; Klausner et al. 2016; Lei et al. 2008).
3. During geomagnetic storms related to HSSs, the low-latitude ionosphere is highly variable, presenting increases and decreases in its density and heights. The ionospheric electron content represented by VTEC can be increased more than 100% over the quiet day average, especially around the southern crest of EIA. During the first geomagnetic storm, occurred in March 2008 and followed by a HILDCAA interval, VTEC showed diurnal and nocturnal intensifications. The deviation from the quiet day variability reached more than ~ 130% over the southern crest of EIA. For the second interval, on April 23, the geomagnetic storm presents the same intensity, Sym H ~ − 45 nT, but less duration than the previous one.

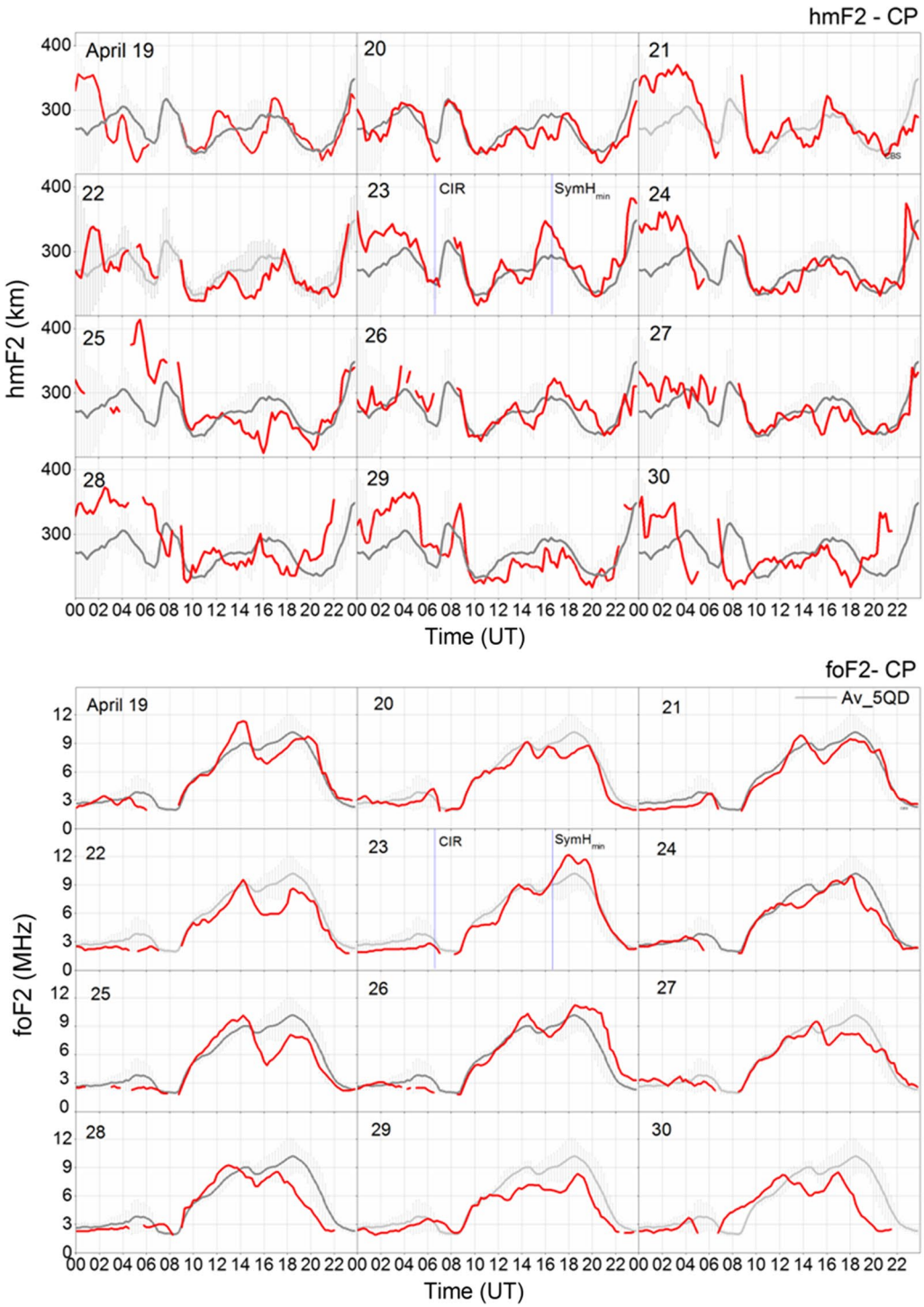

Fig. 13 hmF2 (top panel) and foF2 (bottom panel) variation for the interval April 19 to April 30, from Digisonde measurements at CP

4. Observations at low latitudes using Digisonde e VTEC data showed a phase difference between the F-layer peak height, hmF2, and the Vertical Total Electron Content, VTEC, and the ionospheric plasma critical frequency, foF2, marked by a delay of ~ 2 h, for this period of the year. During the disturbed CIRs/HSSs interval, the hmF2 was higher than those observed during quiet days, which possi-

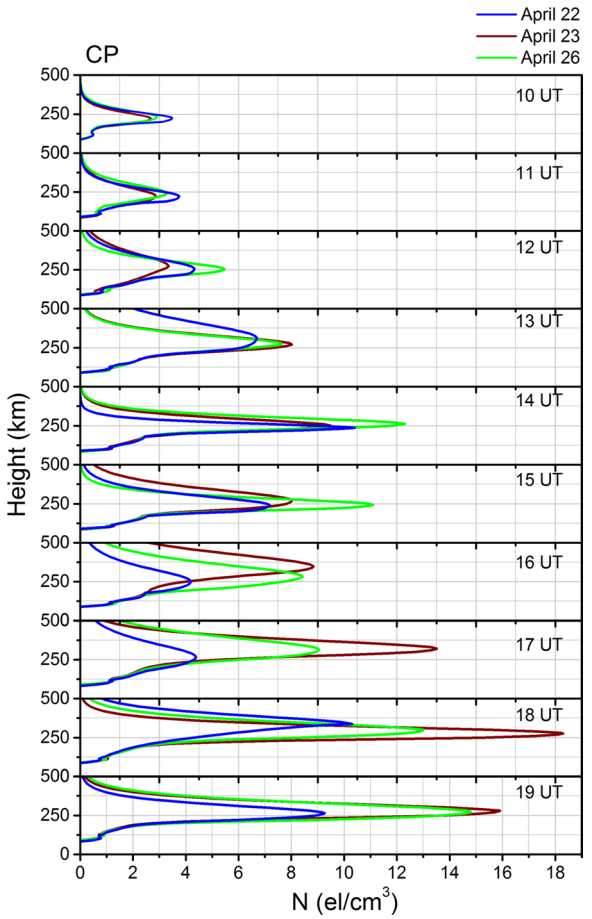

Fig. 14 Vertical electron density profiles from Digisonde measurements at Cachoeira Paulista (22.7°S; 45.0°W), from 10:00 to 19:00 UT for April 22 (quiet day), 23 (disturbed day), and 26 (recovery phase)

bly contributed to the enhanced diurnal ionization. This behavior can be explained by equatorward-disturbed wind, which keeps the F-region at higher altitudes. Additionally, the continuous and oscillatory nature of IMF_Bz, IEF_Ey, and AE could be provided the conditions to reinforce the vertical drift ExB and the Fountain effect at equatorial region, which lead to stronger EIA formation (higher VTEC and foF2).

5. In April, it was observed the occurrence of unusual bite-outs in VTEC and foF2 at low latitudes. The analysis of hmF2, foF2, and the vertical profiles of plasma density taken from data over the EIA showed that vertical expansion and contraction of the F-layer are possible responsible by the occurrence of bite-outs and two diurnal peaks of ionization at low latitudes. This behavior does not seem to be related to the geomagnetic disturbance since it is observed during quiet times as well. However, during disturbed times, the bite-outs can be modified. The mechanisms responsible for the occurrence of bit-outs are not entirely understood and need further investigation.
6. In comparison with the comprehensive study performed by Verkhoglyadova et al. (2011), we should address our findings for the low latitude region in South America. We observed increases in VTEC more than 130% over the quiet time average during the geomagnetic storm in March. This event was noticeable by the occurrence of HILDCAAs which can explain the high variability of VTEC from equatorial to low latitudes around the southern crest of EIA.

Abbreviations

CAS: Chinese Academy of Sciences; NSSC: National Space Science Center (NSSC); INPE: Instituto Nacional de Pesquisas Espaciais; UNIVAP: Universidade do Vale do Paraíba; CRAAM: Centro de Radio Astronomia e Astrofisica Mackenzie; HILDCAASs: high-intensity long-duration continuous auroral activity; CIRs: corotating interaction regions; HSSs: high-speed streams; WHI: whole heliospheric interval; IMF_Bz: North–South component of the interplanetary magnetic field; PPEFs: prompt penetration interplanetary electric fields; VTEC: vertical total electron content; GPS: global navigation system; RBMC: Brazilian Continuous Monitoring Network; IBGE: Brazilian Institute for Geography and Statistics; hmF2: F-layer peak height; foF2: critical plasma frequency; CP: Cachoeira Paulista; GWT: gapped wavelet technique; ICMEs: interplanetary coronal mass ejection; EIA: equatorial ionization anomaly; SAMA: South American/Atlantic Magnetic Anomaly; MSTIDs: mesoscale traveling ionospheric disturbances; GIMs: global ionospheric maps; EPBs: equatorial plasma bubbles; AV5QD: average of the five quietest days; NmF2: maximum plasma density; SALU: Sao Luis; FOR: Fortaleza; GVAL: Governador Valadares; UBAT: Ubatuba; SMAR: Santa Maria; AE: auroral electrojet index; Kp: geomagnetic index; Dst: disturbance storm time index; Vsw: solar wind speed; Np: proton density; Tp: proton temperature; UT: universal time; LT: local time.

Author's contributions

CMNC conceived the study, the majority of the figures, interpretations, and writting and revised the manuscript. ISB provided ionosonde data and helped with the revision of the manuscript. VK contributed to the spectral analysis using wavelet technique and interpretation of the results. PMdeSN has contributed to the GPS data processing and discussion of the results. FBG has contributed with part of the GPS data processing, discussion of the results and revision of the manuscript. ERP and JS have contributed reading the manuscript, with suggestions and of some corrections and discussions. All authors read and approved the final manuscript.

Author details

[1] State Key Laboratory for Space Weather, National Space Science Center (NSSC), Chinese Academy of Sciences (CAS), N°1, Nanertiao, Zhongguancun, Haidian District, Beijing 100190, China. [2] National Institute for Space Research, INPE, Av. dos Astronautas, 1758 – Jardim da Granja, São José dos Campos 12227-010, Brazil. [3] Universidade do Vale do Paraíba, UNIVAP, Av. Dr Shishima Ifumi, 2911 – Urbanova, São José dos Campos, SP 12244-000, Brazil. [4] Centro de Radio Astronomia e Astrofisica Mackenzie, CRAAM, Universidade Presbiteriana Mackenzie, Rua da Consolação 896, São Paulo, SP 01302907, Brazil.

Acknowledgements

The author CMNC would like to thank CAPES, by the financial support, under the contract PNPD20132017-33010013008, CNPq, process 164537/2015-5, and to China-Brazil Joint Laboratory for Space Weather and Chinese Academy of Science (CAS) for the Postdoctoral fellowship, Processes: n. 41474137 and 41674145. The authors thank the Brazilian Network for Continuous Monitoring (RBMC/IBGE) by the GPS-GNSS TEC data and to Solar and Terrestrial

Environment Laboratory (STEL) at Nagoya University and to Dr Gopi Seemala and Boston College by the software to calculate VTEC over South America. We are also grateful to National Space Science Data Center's OmniWeb (http://omniweb.gsfc.nasa.gov), for the solar, interplanetary, and geomagnetic indices and parameters. The authors are also thankful to the technical staff of IBGE and STEL for managing and maintenance of geophysical data. The authors thank to the referees for the constructive comments which improved the content of the manuscript.

Competing Interests
This author declares that she has no competing interests.

Availability of data and materials
Ionospheric data can be found at the following sites: http://www2.inpe.br/climaespacial/portal/en/, TEC data at www.ibge.gov.br/home/geociencias/geodesia/rbmc/rbmc.shtm and with the author CMNC.

Funding
This work was supported by CAPES/PNPD Grant Number 20132017-33010013008, CNPq, Grant Number: 164537/2015-5, China-Brazil Joint laboratory for Space Weather NSSC/INPE/Process: n. 41474137 and n. 41674145.

Publisher's Note

Received: 15 January 2018 Accepted: 13 June 2018
Published online: 28 June 2018

References

Abalde JR, Sahai Y, Fagundes PR, Becker-Guedes F, Bittencourt JA, Pillat VG, Lima WLC, Candido CMN, de Freitas TF (2009) Day-to-day variability in the development of plasma bubbles associated with geomagnetic disturbances. J Geophys Res 114:A04304. https://doi.org/10.1029/2008ja013788

Abdu MA (2005) Equatorial ionosphere-thermosphere system: electrodynamics and irregularities. Adv Space Res 35:771–787

Abdu MA, Kherani EA, Batista IS, de Paula ER, Fritts DC, Sobral JHA (2008) Gravity wave initiation of equatorial spread F/plasma bubble irregularities based on observational data from the SpreadFEx campaign. Ann Geophys 27:2607–2622, 2009

Araujo-Pradere EA, Redmon R, Fedrizzi M, Viereck R, Fuller-Rowell TJ (2011) Some characteristics of the ionospheric behavior during solar cycle 23/24 minimum. Sol Phys 274:439–456. https://doi.org/10.1007/s11207-011-9728-3

Balan N, Shiokawa K, Otsuka Y, Watanabe S, Bailey GJ (2009) Super plasma fountain and equatorial ionization anomaly during penetration electric field. J Geophys Res 114:A03310. https://doi.org/10.1029/2008ja013768

Batista IS, Candido CMN, Souza JR, Abdu MA, de Araujo RC, Resende LCA, Santos AM (2017) F3 layer development during quiet and disturbed periods as observed at conjugate locations in Brazil: the role of the meridional wind. J Geophys Res Space Phys 122:2361–2373. https://doi.org/10.1002/2016ja023724

Bhattacharyya A, Kakad B, Sripathi S, Jeeva K, Nair KU (2014) Development of intermediate scale structure near the peak of the F region within an equatorial plasma bubble. J Geophys Res Space Phys 119:3066–3076. https://doi.org/10.1002/2013ja019619

Burns AG, Solomon SC, Qian L, Wang W, Emery BA, Wiltberger M, Weimer DR (2012) The effects of Corotating interaction region/High-speed stream storms on the thermosphere and ionosphere during the last solar minimum. J Atmos Solar Terr Phys 83:79–87. https://doi.org/10.1016/j.jastp.2012.02.006

Candido CMN, Pimenta AA, Bittencourt JA, Becker-Guedes F (2008) Statistical analysis of the occurrence of medium-scale traveling ionospheric disturbances over Brazilian low latitudes using OI 630.0 nm emission all-sky images. Geophys Res Lett. https://doi.org/10.1029/2008gl035043

Candido CMN, Batista IS, Becker-Guedes F, Abdu MA, Sobral JHA, Takahashi H (2011) Spread F occurrence over a southern anomaly crest location in Brazil during June solstice of solar minimum activity. J Geophys Res 116:A06316. https://doi.org/10.1029/2010ja016374

de Siqueira Negreti PM, de Paula ER, Candido CMN (2017) Total electron content responses to HILDCAAs and geomagnetic storms over South America. Ann Geophys 35:1309–1326. https://doi.org/10.5194/angeo-35-1309-2017

Denton MH, Borovski JE, Horne RB, MCPherron RL, Morley SK, Tsurutani BT (2008) High-speed solar wind streams: a call for key research. Eos 89(7):62–62

Emmert JT, Lean JL, Picone JM (2010) Record-low thermospheric density during the 2008 solar minimum. Geophys Res Lett 37:L12102. https://doi.org/10.1029/2010gl043671

Fejer BG (2011) Low latitude ionospheric electrodynamics. Space Sci Rev 158:145–166. https://doi.org/10.1007/s11214-010-9690-7

Gibson SE, Kozyra JU, de Toma G, Emery BA, Onsager T, Thompson BJ (2009) If the Sun is so quiet, why is the Earth ringing? A comparison of two solar minimum intervals. J Geophys Res 114:A09105. https://doi.org/10.1029/2009ja014342

Gray LJ, Beer J, Geller M, Haigh JD, Lockwood M, Matthes K, Cubasch U, Fleitmann D, Harrison G, Hood L, Luterbacher J, Meehl GA, Shindell D, van Geel B, White W (2010) Solar influences on climate. Rev Geophys 48:RG4001. https://doi.org/10.1029/2009rg000282

Hajra R, Echer E, Tsurutani BT, Gonzalez WD (2013) Solar cycle dependence of High-Intensity Long-Duration Continuous AE Activity (HILDCAA) events, relativistic electron predictors? J Geophys Res Space Phys 118:5626–5638. https://doi.org/10.1002/jgra.50530

Harvey JW (2013) The Sun in time. Space Sci Rev. https://doi.org/10.1007/s11214-010-9726-z

Klausner V, Papa ARR, Mendes O, Domingues MO, Frick P (2013) Characteristics of solar diurnal variations: a case study based on records from the ground magnetic station at Vassouras, Brazil. J Atmos Solar Terr Phys 92:124–136. https://doi.org/10.1016/j.jastp.2012.10.007

Klausner V, Papa ARR, Candido CMN, Domingues MO, Mendes O (2016) An alternative way to identify local geomagnetically quiet days: a case study using wavelet analysis. Ann Geophys 34:451–462. https://doi.org/10.5194/angeo-34-451-2016

Klenzing J, Simões F, Ivanov S, Heelis RA, Bilitza D, Pfaff R, Rowland D (2011) Topside equatorial ionospheric density and composition during and after extreme solar minimum. J Geophys Res 116:A12330. https://doi.org/10.1029/2011ja017213

Koga D, Sobral JHA, Abdu MA, de Castilho VM, Mascarenhas M, Arruda DCS, Zamlutti CJ, Takahashi H, Medeiros AF, Buriti RA (2011) Space weather in the thermospheric–ionospheric domain over the Brazilian region: climatology of ionospheric plasma bubbles in the subequatorial and low-latitude region. J Atmos Solar Terr Phys 73(11–12):1529–1534. https://doi.org/10.1016/j.jastp.2010.08.017

Lee CC (2012) Examination of the absence of noontime bite-out in equatorial total electron content. J Geophys Res 117:A09303. https://doi.org/10.1029/2012ja017909

Lei J, Thayer JP, Forbes JM, Wu Q, She C, Wan W, Wang W (2008) Ionosphere response to solar wind high-speed streams. Geophys Res Lett 35:L19105. https://doi.org/10.1029/2008gl035208

Liu J, Liu L, Zhao B, Wei Y, Hu L, Xiong B (2012) High-speed stream impacts on the equatorial ionization anomaly region during the deep solar minimum year 2008. J Geophys Res 117:A10304. https://doi.org/10.1029/2012ja018015

Mannucci AJ, Tsurutani BT, Kelley MC, Iijma BA, Komjathy A (2009) Local time dependence of the prompt penetration response for 7, 9 and 10 November 2004 superstorms. J Geophys Res 114:A10308. https://doi.org/10.1029/2009ja014043

Otsuka Y, Ogawa T, Saito A, Tsugawa T, Fukao S, Miyazaki S (2002) A new technique for mapping of total electron content using GPS network in Japan. Earth Planets Space 54:63–70. https://doi.org/10.1186/BF03352422

Pedatella NM, Forbes JM (2011) Electrodynamic response of the ionosphere to high-speed solar wind streams. J Geophys Res 116:A12310. https://doi.org/10.1029/2011ja017050

Rajaram G, Rastogi RG (1977) Equatorial electron densities seasonal and solar cycle changes. J Atmos Solar Terr Phys 39:1175–1182. https://doi.org/10.1016/0021-9169(77)90026-5

Reinisch BW, Huang X, Galkin IA, Paznukhov V, Kozlov A (2005) Recent advances in real-time analysis of ionograms and ionospheric drift measurements with digisondes. J Atmos Solar Terr Phys 67:1054–1062

Schwadron NA, Spence HE, Came R (2011) Does the space environment affect the ecosphere? Eos 92(36):297–298

Seemala GK, Valladares CE (2011) Statistics of total electron content depletions observed over the South American continent for the year 2008. Radio Sci 46:RS5019. https://doi.org/10.1029/2011rs004722

Sobral JHA, Abdu MA, Takahashi H, Taylor MJ, de Paula ER, Zamlutti CJ, Borba GL (2002) A study of the ionospheric plasma bubbles climatology over Brazil, based on 22 years (1977–1998) of OI 630 nm airglow observation. J Atmos Solar Terr Phys 64(12–14):1517–1524. https://doi.org/10.1016/s1364-6826(02)00089-5

Solomon SC, Qian L, Burns AG (2013) The anomalous ionosphere between solar cycles 23 and 24. J Geophys Res Space Phys 118:6524–6535. https://doi.org/10.1002/jgra.50561

Tsurutani BT, Gonzalez WD, Gonzalez ALC, Guarnieri FL, Gopalswamy N, Grande M, Kamide Y, Kasahara Y, Lu G, McPherron R, Soraas F, Vasyliunas V (2006) Corotating solar wind streams and recurrent geomagnetic activity: a review. J Geophys Res 111:A07S01. https://doi.org/10.1029/2005ja011273

Tulasi Ram S, Lei J, Su S-Y, Liu CH, Lin CH, Chen WS (2010) Dayside ionospheric response to recurrent geomagnetic activity during the extreme solar minimum of 2008. Geophys Res Lett 37:L02101. https://doi.org/10.1029/2009gl041038

Tulasi Ram S, Yamamoto M, Veenadhari B, Sandeep Kumar, Gurubaran S (2012) Corotating interaction regions (CIRs) at sub-harmonics solar rotational periods and their impact on ionosphere-thermosphere system during the extreme low solar activity year 2008. Indian J Radio Space 41:294–305

Venkatesh K, Fagundes PR, de Abreu AJ, Pillat VG (2016) Unusual noon-time bite-outs in the ionospheric electron density around the anomaly crest locations overt the Indian and Brazilian sectors during quiet time conditions—a case study. J Atmos Solar Terr Phys 147:126–237. https://doi.org/10.1016/j.jastp.2016.07.016

Verkhoglyadova OP, Tsurutani BT, Mannucci AJ, Mlynczak MG, Hunt LA, Komjathy A, Runge T (2011) Ionospheric VTEC and thermospheric infrared emission dynamics during corotating interaction region and high-speed stream intervals at solar minimum: 25 March to 26 April 2008. J Geophys Res 116:A09325. https://doi.org/10.1029/2011ja016604

Verkhoglyadova OP, Tsurutani BT, Mannucci AJ, Mlynczak MG, Hunt LA, Runge T (2013) Variability of ionospheric TEC during solar and geomagnetic minima (2008 and 2009): external high-speed stream drivers. Ann Geophys 31:263–276

Wang W, Lei J, Burns AG, Qian L, Solomon SC, Wiltberger M, Xu J (2011) Ionospheric day-to-day variability around the whole heliosphere interval in 2008. Sol Phys 274(1–2):457–472. https://doi.org/10.1007/s11207-11-9747-0

Xystouris G, Sigala E, Mavromichalaki H (2014) A complete catalog of high speed solar wind streams during solar cycle 23. Sol Phys 289:995–1012. https://doi.org/10.1007/s11207-013-0355-z